

Search for electroweak production of single top quarks in $p\bar{p}$ collisions

B. Abbott,⁵⁰ M. Abolins,⁴⁷ V. Abramov,²³ B. S. Acharya,¹⁵ D. L. Adams,⁵⁷ M. Adams,³⁴ G. A. Alves,² N. Amos,⁴⁶ E. W. Anderson,³⁹ M. M. Baarmand,⁵² V. V. Babintsev,²³ L. Babukhadia,⁵² A. Baden,⁴³ B. Baldin,³³ P. W. Balm,¹⁸ S. Banerjee,¹⁵ J. Bantly,⁵⁶ E. Barberis,²⁶ P. Baringer,⁴⁰ J. F. Bartlett,³³ U. Bassler,¹¹ A. Bean,⁴⁰ M. Begel,⁵¹ A. Belyaev,²² S. B. Beri,¹³ G. Bernardi,¹¹ I. Bertram,²⁴ A. Besson,⁹ V. A. Bezzubov,²³ P. C. Bhat,³³ V. Bhatnagar,¹³ M. Bhattacharjee,⁵² G. Blazey,³⁵ S. Blessing,³¹ A. Boehnlein,³³ N. I. Bojko,²³ E. E. Boos,²² F. Borchering,³³ A. Brandt,⁵⁷ R. Breedon,²⁷ G. Briskin,⁵⁶ R. Brock,⁴⁷ G. Brooijmans,³³ A. Bross,³³ D. Buchholz,³⁶ M. Buehler,³⁴ V. Buescher,⁵¹ V. S. Burtovoi,²³ J. M. Butler,⁴⁴ F. Canelli,⁵¹ W. Carvalho,³ D. Casey,⁴⁷ Z. Casilum,⁵² H. Castilla-Valdez,¹⁷ D. Chakraborty,⁵² K. M. Chan,⁵¹ S. V. Chekulaev,²³ D. K. Cho,⁵¹ S. Choi,³⁰ S. Chopra,⁵³ J. H. Christenson,³³ M. Chung,³⁴ D. Claes,⁴⁸ A. R. Clark,²⁶ J. Cochran,³⁰ L. Coney,³⁸ B. Connolly,³¹ W. E. Cooper,³³ D. Coppage,⁴⁰ M. A. C. Cummings,³⁵ D. Cutts,⁵⁶ O. I. Dahl,²⁶ G. A. Davis,⁵¹ K. Davis,²⁵ K. De,⁵⁷ K. Del Signore,⁴⁶ M. Demarteau,³³ R. Demina,⁴¹ P. Demine,⁹ D. Denisov,³³ S. P. Denisov,²³ S. Desai,⁵² H. T. Diehl,³³ M. Diesburg,³³ G. Di Loreto,⁴⁷ S. Doulas,⁴⁵ P. Draper,⁵⁷ Y. Ducros,¹² L. V. Dudko,²² S. Duensing,¹⁹ S. R. Dugad,¹⁵ A. Dyshkant,²³ D. Edmunds,⁴⁷ J. Ellison,³⁰ V. D. Elvira,³³ R. Engelmann,⁵² S. Eno,⁴³ G. Eppley,⁵⁹ P. Ermolov,²² O. V. Eroshin,²³ J. Estrada,⁵¹ H. Evans,⁴⁹ V. N. Evdokimov,²³ T. Fahland,²⁹ S. Feher,³³ D. Fein,²⁵ T. Ferbel,⁵¹ H. E. Fisk,³³ Y. Fisyak,⁵³ E. Flattum,³³ F. Fleuret,²⁶ M. Fortner,³⁵ K. C. Frame,⁴⁷ S. Fuess,³³ E. Gallas,³³ A. N. Galyaev,²³ P. Gartung,³⁰ V. Gavrilov,²¹ R. J. Genik II,²⁴ K. Genser,³³ C. E. Gerber,³⁴ Y. Gershtein,⁵⁶ B. Gibbard,⁵³ R. Gilmartin,³¹ G. Ginther,⁵¹ B. Gómez,⁵ G. Gómez,⁴³ P. I. Goncharov,²³ J. L. González Solís,¹⁷ H. Gordon,⁵³ L. T. Goss,⁵⁸ K. Gounder,³⁰ A. Goussiou,⁵² N. Graf,⁵³ G. Graham,⁴³ P. D. Grannis,⁵² J. A. Green,³⁹ H. Greenlee,³³ S. Grinstein,¹ L. Groer,⁴⁹ P. Grudberg,²⁶ S. Grünendahl,³³ A. Gupta,¹⁵ S. N. Gurzhiev,²³ G. Gutierrez,³³ P. Gutierrez,⁵⁵ N. J. Hadley,⁴³ H. Haggerty,³³ S. Hagopian,³¹ V. Hagopian,³¹ K. S. Hahn,⁵¹ R. E. Hall,²⁸ P. Hanlet,⁴⁵ S. Hansen,³³ J. M. Hauptman,³⁹ C. Hays,⁴⁹ C. Hebert,⁴⁰ D. Hedin,³⁵ A. P. Heinson,³⁰ U. Heintz,⁴⁴ T. Heuring,³¹ R. Hirosky,³⁴ J. D. Hobbs,⁵² B. Hoeneisen,⁸ J. S. Hoftun,⁵⁶ S. Hou,⁴⁶ Y. Huang,⁴⁶ A. S. Ito,³³ S. A. Jerger,⁴⁷ R. Jesik,³⁷ K. Johns,²⁵ M. Johnson,³³ A. Jonckheere,³³ M. Jones,³² H. Jöstlein,³³ A. Juste,³³ S. Kahn,⁵³ E. Kajfasz,¹⁰ D. Karmanov,²² D. Karmgard,³⁸ R. Kehoe,³⁸ S. K. Kim,¹⁶ B. Klima,³³ C. Klopfenstein,²⁷ B. Knuteson,²⁶ W. Ko,²⁷ J. M. Kohli,¹³ A. V. Kostitskiy,²³ J. Kotcher,⁵³ A. V. Kotwal,⁴⁹ A. V. Kozelov,²³ E. A. Kozlovsky,²³ J. Krane,³⁹ M. R. Krishnaswamy,¹⁵ S. Krzywdzinski,³³ M. Kubantsev,⁴¹ S. Kuleshov,²¹ Y. Kulik,⁵² S. Kunori,⁴³ V. E. Kuznetsov,³⁰ G. Landsberg,⁵⁶ A. Leflat,²² F. Lehner,³³ J. Li,⁵⁷ Q. Z. Li,³³ J. G. R. Lima,³ D. Lincoln,³³ S. L. Linn,³¹ J. Linnemann,⁴⁷ R. Lipton,³³ A. Lucotte,⁵² L. Lueking,³³ C. Lundstedt,⁴⁸ A. K. A. Maciel,³⁵ R. J. Madaras,²⁶ V. Manankov,²² H. S. Mao,⁴ T. Marshall,³⁷ M. I. Martin,³³ R. D. Martin,³⁴ K. M. Mauritz,³⁹ B. May,³⁶ A. A. Mayorov,³⁷ R. McCarthy,⁵² J. McDonald,³¹ T. McMahon,⁵⁴ H. L. Melanson,³³ X. C. Meng,⁴ M. Merkin,²² K. W. Merritt,³³ C. Miao,⁵⁶ H. Miettinen,⁵⁹ D. Mihalcea,⁵⁵ A. Mincer,⁵⁰ C. S. Mishra,³³ N. Mokhov,³³ N. K. Mondal,¹⁵ H. E. Montgomery,³³ R. W. Moore,⁴⁷ M. Mostafa,¹ H. da Motta,⁴⁶ E. Nagy,¹⁰ F. Nang,²⁵ M. Narain,⁴⁴ V. S. Narasimham,¹⁵ H. A. Neal,⁴⁶ J. P. Negret,⁵ S. Negroni,¹⁰ D. Norman,⁵⁸ L. Oesch,⁴⁶ V. Oguri,³ B. Olivier,¹¹ N. Oshima,³³ P. Padley,⁵⁹ L. J. Pan,³⁶ A. Para,³³ N. Parashar,⁴⁵ R. Partridge,⁵⁶ N. Parua,⁹ M. Paterno,⁵¹ A. Patwa,⁵² B. Pawlik,²⁰ J. Perkins,⁵⁷ M. Peters,³² O. Peters,¹⁸ R. Piegaia,¹ H. Piekarczyk,³¹ B. G. Pope,⁴⁷ E. Popkov,³⁸ H. B. Prosper,³¹ S. Protopopescu,⁵³ J. Qian,⁴⁶ P. Z. Quintas,³³ R. Raja,⁵³ S. Rajagopalan,⁵³ E. Ramberg,³³ P. A. Rapidis,³³ N. W. Reay,⁴¹ S. Reucroft,⁴⁵ J. Rha,³⁰ M. Rijssenbeek,⁵² T. Rockwell,⁴⁷ M. Roco,³³ P. Rubinov,³³ R. Ruchti,³⁸ J. Rutherford,²⁵ A. Santoro,² L. Sawyer,⁴² R. D. Schamberger,⁵² H. Schellman,³⁶ A. Schwartzman,¹ J. Sculli,⁵⁰ N. Sen,⁵⁹ E. Shabalina,²² H. C. Shankar,¹⁵ R. K. Shivpuri,¹⁴ D. Shpakov,⁵² M. Shupe,²⁵ R. A. Sidwell,⁴¹ V. Simak,⁷ H. Singh,³⁰ J. B. Singh,¹³ V. Sirotenko,³³ P. Slattery,⁵¹ E. Smith,⁵⁵ R. P. Smith,³³ R. Snihur,³⁶ G. R. Snow,⁴⁸ J. Snow,⁵⁴ S. Snyder,⁵³ J. Solomon,³⁴ V. Sorin,¹ M. Sosebee,⁵⁷ N. Sotnikova,²² K. Soustruznik,⁶ M. Souza,² N. R. Stanton,⁴¹ G. Steinbrück,⁴⁹ R. W. Stephens,⁵⁷ M. L. Stevenson,²⁶ F. Stichelbaut,⁵³ D. Stoker,²⁹ V. Stolin,²¹ D. A. Stoyanova,²³ M. Strauss,⁵⁵ K. Streets,⁵⁰ M. Strovink,²⁶ L. Stutte,³³ A. Sznajder,³ W. Taylor,⁵² S. Tentindo-Repond,³¹ J. Thompson,⁴³ D. Toback,⁴³ S. M. Tripathi,²⁷ T. G. Trippe,²⁶ A. S. Turcot,⁵³ P. M. Tuts,⁴⁹ P. van Gemmeren,³³ V. Vaniev,²³ R. Van Kooten,³⁷ N. Varelas,³⁴ A. A. Volkov,²³ A. P. Vorobiev,²³ H. D. Wahl,³¹ H. Wang,³⁶ Z.-M. Wang,⁵² J. Warchol,³⁸ G. Watts,⁶⁰ M. Wayne,³⁸ H. Weerts,⁴⁷ A. White,⁵⁷ J.T. White,⁵⁸ D. Whiteson,²⁶ J. A. Wightman,³⁹ D. A. Wijngaarden,¹⁹ S. Willis,³⁵ S. J. Wimpenny,³⁰ J. V. D. Wirjawan,⁵⁸ J. Womersley,³³ D. R. Wood,⁴⁵ R. Yamada,³³ P. Yamin,⁵³ T. Yasuda,³³ K. Yip,³³ S. Youssef,³¹ J. Yu,³³ Z. Yu,³⁶ M. Zanabria,⁵ H. Zheng,³⁸ Z. Zhou,³⁹ Z. H. Zhu,⁵¹ M. Zielinski,⁵¹ D. Zieminska,³⁷ A. Zieminski,³⁷ V. Zutshi,⁵¹ E. G. Zverev,²² and A. Zylberstein¹²

(DØ Collaboration)

¹Universidad de Buenos Aires, Buenos Aires, Argentina²LAFEX, Centro Brasileiro de Pesquisas Físicas, Rio de Janeiro, Brazil³Universidade do Estado do Rio de Janeiro, Rio de Janeiro, Brazil⁴Institute of High Energy Physics, Beijing, People's Republic of China⁵Universidad de los Andes, Bogotá, Colombia⁶Charles University, Prague, Czech Republic⁷Institute of Physics, Academy of Sciences, Prague, Czech Republic⁸Universidad San Francisco de Quito, Quito, Ecuador

- ⁹*Institut des Sciences Nucléaires, IN2P3-CNRS, Université de Grenoble I, Grenoble, France*
¹⁰*CPPM, IN2P3-CNRS, Université de la Méditerranée, Marseille, France*
¹¹*LPNHE, Universités Paris VI and VII, IN2P3-CNRS, Paris, France*
¹²*DAPNIA/Service de Physique des Particules, CEA, Saclay, France*
¹³*Panjab University, Chandigarh, India*
¹⁴*Delhi University, Delhi, India*
¹⁵*Tata Institute of Fundamental Research, Mumbai, India*
¹⁶*Seoul National University, Seoul, Korea*
¹⁷*CINVESTAV, Mexico City, Mexico*
¹⁸*FOM-Institute NIKHEF and University of Amsterdam/NIKHEF, Amsterdam, The Netherlands*
¹⁹*University of Nijmegen/NIKHEF, Nijmegen, The Netherlands*
²⁰*Institute of Nuclear Physics, Kraków, Poland*
²¹*Institute for Theoretical and Experimental Physics, Moscow, Russia*
²²*Moscow State University, Moscow, Russia*
²³*Institute for High Energy Physics, Protvino, Russia*
²⁴*Lancaster University, Lancaster, United Kingdom*
²⁵*University of Arizona, Tucson, Arizona 85721*
²⁶*Lawrence Berkeley National Laboratory and University of California, Berkeley, California 94720*
²⁷*University of California, Davis, California 95616*
²⁸*California State University, Fresno, California 93740*
²⁹*University of California, Irvine, California 92697*
³⁰*University of California, Riverside, California 92521*
³¹*Florida State University, Tallahassee, Florida 32306*
³²*University of Hawaii, Honolulu, Hawaii 96822*
³³*Fermi National Accelerator Laboratory, Batavia, Illinois 60510*
³⁴*University of Illinois at Chicago, Chicago, Illinois 60607*
³⁵*Northern Illinois University, DeKalb, Illinois 60115*
³⁶*Northwestern University, Evanston, Illinois 60208*
³⁷*Indiana University, Bloomington, Indiana 47405*
³⁸*University of Notre Dame, Notre Dame, Indiana 46556*
³⁹*Iowa State University, Ames, Iowa 50011*
⁴⁰*University of Kansas, Lawrence, Kansas 66045*
⁴¹*Kansas State University, Manhattan, Kansas 66506*
⁴²*Louisiana Tech University, Ruston, Louisiana 71272*
⁴³*University of Maryland, College Park, Maryland 20742*
⁴⁴*Boston University, Boston, Massachusetts 02215*
⁴⁵*Northeastern University, Boston, Massachusetts 02115*
⁴⁶*University of Michigan, Ann Arbor, Michigan 48109*
⁴⁷*Michigan State University, East Lansing, Michigan 48824*
⁴⁸*University of Nebraska, Lincoln, Nebraska 68588*
⁴⁹*Columbia University, New York, New York 10027*
⁵⁰*New York University, New York, New York 10003*
⁵¹*University of Rochester, Rochester, New York 14627*
⁵²*State University of New York, Stony Brook, New York 11794*
⁵³*Brookhaven National Laboratory, Upton, New York 11973*
⁵⁴*Langston University, Langston, Oklahoma 73050*
⁵⁵*University of Oklahoma, Norman, Oklahoma 73019*
⁵⁶*Brown University, Providence, Rhode Island 02912*
⁵⁷*University of Texas, Arlington, Texas 76019*
⁵⁸*Texas A&M University, College Station, Texas 77843*
⁵⁹*Rice University, Houston, Texas 77005*
⁶⁰*University of Washington, Seattle, Washington 98195*

(Received 16 August 2000; published 29 December 2000)

We present a search for electroweak production of single top quarks in the electron+jets and muon+jets decay channels. The measurements use $\approx 90 \text{ pb}^{-1}$ of data from Run 1 of the Fermilab Tevatron collider, collected at 1.8 TeV with the DØ detector between 1992 and 1995. We use events that include a tagging muon, implying the presence of a b jet, to set an upper limit at the 95% confidence level on the cross section for the s -channel process $p\bar{p} \rightarrow t\bar{b} + X$ of 39 pb. The upper limit for the t -channel process $p\bar{p} \rightarrow tq\bar{b} + X$ is 58 pb.

The top quark is the charge $+2/3$ weak-isospin partner of the bottom quark in the third generation of fermions of the standard model (SM). It is extremely massive at 174.3 ± 5.1 GeV [1], and, with an expected width of 1.5 GeV [2], it decays before hadronization almost exclusively into a W boson and a b quark. At the Fermilab Tevatron $p\bar{p}$ collider, most top quarks are pair-produced via the strong interaction through an intermediate gluon. This was the mode used in its observation [3] and subsequent studies of its properties, including measurements of the $t\bar{t}$ production cross section of 5.9 ± 1.7 pb by the $D\bar{O}$ Collaboration [4], and $6.5^{+1.7}_{-1.4}$ pb by the Collider Detector at Fermilab (CDF) Collaboration [5]. A second production mode is predicted to exist, where top quarks are created singly through an electroweak Wtb vertex [6]. Many processes beyond the SM can boost the single top quark cross section [7]. In the absence of a cross section excess, measurement of the electroweak production of single top quarks could provide the magnitude of the Cabibbo-Kobayashi-Maskawa (CKM) matrix element V_{tb} [8] since the cross section is proportional to $|V_{tb}|^2$. In this Rapid Communication, we describe a search for single top quarks at the Tevatron using data collected from 1992–1995 at a $p\bar{p}$ center-of-mass energy of 1.8 TeV.

The standard model predicts three modes for the production of single top quarks at a hadron collider. The first is the s -channel process $q'\bar{q} \rightarrow tb$, illustrated in Fig. 1(a). For a top quark mass m_t of 175 GeV, this has a cross section calculated at next-to-leading-order (NLO) of 0.73 ± 0.10 pb [9]. Following the decay of the top quark, these events contain a W boson and two b quarks that hadronize into two central jets with high transverse momentum (p_T). The second production mode, shown in Fig. 1(b) and sometimes referred to as W -gluon fusion, is a t -channel process, $q'g \rightarrow tqb$. The NLO cross section is 1.70 ± 0.24 pb [10]. This process produces a W boson, a forward light-quark jet, and two central b jets, one with high p_T and the other with low p_T . We have searched for both production modes, with decay of the W boson into $e\nu$ or $\mu\nu$, and identification of a b jet via a tagging muon. A third mode occurs via both the s -channel and t -channel, $bg \rightarrow tW$, with a final state containing two W bosons and a single b jet. The leading-order cross section for this process is only 0.15 pb [11], and, with ≈ 90 pb^{-1} of available data, there is no possibility of separating it from the background. Throughout this paper, we use “ tb ” to refer to both $t\bar{b}$ and the charge-conjugate process $\bar{t}b$, and “ tqb ” to both $tq\bar{b}$ and $\bar{t}qb$.

The $D\bar{O}$ detector [12] has three major components: a central tracking system including a transition radiation detector (TRD), a uranium/liquid-argon calorimeter, and a muon spectrometer. For the measurement in the electron channel, we use 91.9 ± 4.1 pb^{-1} of data collected with a trigger that required an electromagnetic (EM) energy cluster in the calorimeter, a jet, and missing transverse momentum (\cancel{E}_T). For events passing the final selection, the efficiency of the trigger is 90–93%, depending on the location of the EM cluster in the calorimeter. In the muon channel, we use 88.0 ± 3.9 pb^{-1} of data acquired with several triggers, which re-

quired \cancel{E}_T or a muon with a jet. The combined efficiency of these triggers is 96–99%. A third data sample, obtained with a trigger requiring just three jets, is used for measuring one of the backgrounds. Since the multijet cross section is very large, this trigger was prescaled, and we have 0.8 pb^{-1} of such data. Each of the three samples contains approximately one million events.

To determine whether an EM energy cluster was generated by an electron, we require it to be isolated from other activity in the calorimeter and use a five-variable likelihood function to discriminate electrons from the background. This likelihood includes the fraction of cluster energy contained in the EM region of the calorimeter ($>90\%$ for electrons), the cluster shape (it must resemble an electron and not a pion), the presence of a well-matched track between the cluster and a primary $p\bar{p}$ interaction vertex (to discriminate against photons), the dE/dx energy loss along the track (consistent with a single particle and not from a photon conversion into a pair of charged particles), and the TRD response (matching that of an electron and not a pion). An electron is then required to have transverse energy $E_T > 20$ GeV, and to be within the optimal region of the calorimeters with detector pseudorapidity $|\eta^{\text{det}}| < 1.1$ or $1.5 < |\eta^{\text{det}}| < 2.5$ [13]. When an electron is isolated, it is more likely to have originated from the decay of a W boson than from a b hadron. The efficiency of the combined electron identification requirements is $\approx 60\%$.

Jets, reconstructed with a cone algorithm of radius $R = 0.5$ [14], must fail the electron requirements. The jet with the highest transverse energy is required to have $E_T > 15$ GeV and $|\eta^{\text{det}}| < 3.0$. The second jet has to have $E_T > 10$ GeV and $|\eta^{\text{det}}| < 4.0$. Other jets in the event are counted if they have $E_T > 5$ GeV and $|\eta^{\text{det}}| < 4.0$. We set the E_T thresholds low and the $|\eta^{\text{det}}|$ region wide to maximize acceptance for signal; however, the efficiency to reconstruct jets close to the 5 GeV threshold is low.

We identify a muon by the pattern of hits in the spectrometer drift tubes, and require an impact parameter < 20 cm between the spectrometer track and the primary vertex, a matching track in the calorimeter consistent with a minimum-ionizing particle, a matching central track, a signal in the scintillators surrounding the spectrometer within ± 12 ns of the beam-crossing time, and penetration through one of the spectrometer toroids for momentum analysis. Most of these requirements are designed to reject cosmic rays and particles backscattered from the beamline magnets. Muons must be within the central region of the spectrometer, with $|\eta^{\text{det}}| < 1.7$. A muon is called “isolated” if $\Delta R(\mu, \text{jet}) \geq 0.5$ [15] for all jets with $E_T > 5$ GeV. An isolated muon must

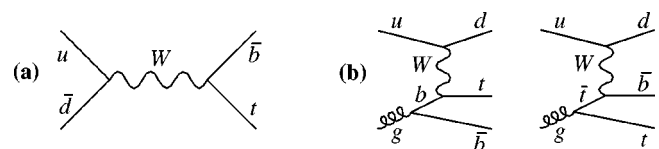


FIG. 1. Leading order Feynman diagrams for single top quark production at the Tevatron, where (a) shows the s -channel mode, and (b) the t -channel mode.

have $p_T > 20$ GeV and is attributed to the decay of a W boson. A “tagging” muon has $\Delta R < 0.5$ and $p_T > 4$ GeV. It is attributed to the semileptonic decay of a b hadron in a jet, and thus identifies a b jet. The efficiency of the combined muon identification requirements is $\approx 44\%$ for isolated muons.

Because a leptonically-decaying W boson is supposed to be present in each signal event, we require $\cancel{E}_T > 15$ GeV as evidence of a neutrino.

We use the NLO single top quark production cross sections to estimate that about 66 s -channel and 153 t -channel events were produced at $D\bar{D}$ during Run 1. Of these, we expect that about 15 s -channel and 35 t -channel events passed the trigger requirements and were recorded for analysis.

Our analysis starts with a simple baseline selection of events that pass the triggers and have at least one reconstructed electron or isolated muon, and at least two jets with $E_T > 5$ GeV and $|\eta^{\text{det}}| < 4.0$. For the results presented in this Rapid Communication, we also demand at least one tagging muon (“ $/\mu$ ”) to indicate the possible presence of a b jet. These minimal requirements reduce the ≈ 1 million events in each channel to 116 $e + \text{jets}/\mu$ events and 110 $\mu + \text{jets}/\mu$ events. The acceptance for single top quark events for these selections is 0.2–0.3% per channel, which should yield ≈ 1 tagged event (tb and tqb , with electron and muon W decays combined). The expected number of events is small because the probability to identify at least one tagging muon in a single top quark event is only 6–11%. After these selections, 90% of the background in the electron channel is from QCD multijet production with a jet misidentified as an electron, 5% from $t\bar{t}$ events, and 5% from $W + \text{jets}$ (including WW and WZ diboson events), where about two thirds of the $W + \text{jets}$ events have a light quark or gluon jet with a false tagging muon, and a quarter of the tagging muons are from c quark decays. In the muon channel, the background is 8% from $W + \text{jets}$ events, 6% from QCD $b\bar{b}$ events where a muon from a b decay mimics an isolated muon, and 4% from $t\bar{t}$ events. The remaining 82% of the background is from QCD multijet events with a coincident cosmic ray or beam-halo particle misidentified as an isolated muon.

Next, we apply a set of loose criteria to remove mismeasured events and to reject backgrounds that do not have the same final-state characteristics as our signal. We reject events with more than one isolated lepton and any isolated photons. We remove events with \cancel{E}_T close to 15 GeV and aligned with or opposite to a jet, or opposite an electron or isolated muon. We also reject events that have muons with clearly mismeasured p_T . We require two, three, or four jets. To remove the remaining contamination from cosmic rays in the isolated muon channel, we reject events where the isolated muon and tagging muon are back-to-back; in particular, we require $\Delta\phi(\text{isol } \mu, \text{tag } \mu) < 2.4$ rad. These criteria, together with the jet E_T and $|\eta^{\text{det}}|$ requirements and the \cancel{E}_T threshold, reject 86% of the baseline multijet “electron” events, 95% of the cosmic ray and misreconstructed isolated “muon” events, 90% of the $b\bar{b}$ “isolated” muon events,

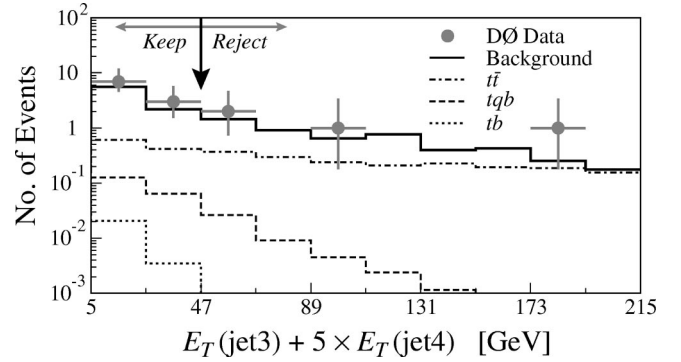


FIG. 2. Variable used to reject the $t\bar{t}$ background.

27% of the $W + \text{jets}$ events in the electron channel, 81% in the muon channel, and 55–73% of the $t\bar{t}$ background. The signal acceptances are reduced by 14–51%. There remain 21 $e + \text{jets}/\mu$ and 8 $\mu + \text{jets}/\mu$ candidates in the data.

Based on independent studies (see below), we apply the following requirements to obtain the best significance of signal over square-root of background in each channel:

Electron Channel

$$\begin{aligned} E_T(\text{jet1}) + E_T(\text{jet2}) + E_T(e) + \cancel{E}_T &> 125 \text{ GeV} \\ E_T(\text{jet3}) + 5 \times E_T(\text{jet4}) &< 47 \text{ GeV} \\ E_T(\text{jet1}) + 4 \times \cancel{E}_T &> 155 \text{ GeV} \end{aligned}$$

Muon Channel

$$\begin{aligned} E_T(\text{jet1}) + E_T(\text{jet2}) + E_T(\text{jet3}) + E_T(\text{jet4}) &> 70 \text{ GeV} \\ E_T(\text{jet3}) + 5 \times E_T(\text{jet4}) &< 47 \text{ GeV} \end{aligned}$$

The first criterion in each set was chosen by studying reconstructed CompHEP [16] Monte Carlo (MC) $W + \text{jets}$ events, the second by examining HERWIG [17] $t\bar{t}$ MC events, and the third variable in the electron channel was determined from studies of QCD multijet data. The distributions were compared with signal MC events from CompHEP. The cutoffs were optimized on combined samples of untagged and tagged events. Figure 2 shows the distribution of the second variable, designed to minimize the $t\bar{t}$ background, for electron and muon events combined after all other selections have been applied.

After final selections, there is no evidence of an excess of signal over background, and we therefore use the results to set limits on the s -channel and t -channel single top quark cross sections. To do this, we must first determine the signal acceptance and the background in each channel.

We obtain the signal acceptances using MC samples of s -channel and t -channel single top quark events from the CompHEP event generator, with the PYTHIA package [18] used to simulate fragmentation, initial-state and final-state radiation, the underlying event, and leptonic decays of the W boson. The MC events are processed through a detector simulation program based on the GEANT [19] package and a trigger simulation, and are then reconstructed. We apply all selections directly to the reconstructed MC events, except for several particle identification criteria, which we correct using factors measured in other $D\bar{D}$ data. Table I shows the acceptance for single top quark events after all selection requirements and corrections.

TABLE I. Signal acceptances (as percentages of the total cross sections) and numbers of events expected to remain after application of all selection criteria.

	Electron Channel	Muon Channel
	Acceptances	
tb	$(0.255 \pm 0.022)\%$	$(0.112 \pm 0.011)\%$
tqb	$(0.168 \pm 0.015)\%$	$(0.083 \pm 0.008)\%$
	Numbers of Events	
tb	0.18 ± 0.03	0.08 ± 0.01
tqb	0.28 ± 0.05	0.13 ± 0.03
$W + \text{jets}$	5.59 ± 0.64	1.12 ± 0.17
QCD	5.92 ± 0.58	0.40 ± 0.09
$t\bar{t}$	1.14 ± 0.35	0.45 ± 0.14
Total Bkgd	12.65 ± 0.93	1.97 ± 0.24
Data	12	5

The acceptance for $t\bar{t}$ pairs is calculated in a manner similar to that for signal and then converted to a number of events using the integrated luminosity for each channel and $D\Phi$'s value of the $t\bar{t}$ cross section [4].

The QCD multijet background with a jet misidentified as an electron is measured using multijet data. The events are weighted by the probability that a jet mimics an electron for each jet that passes the electron E_T and $|\eta^{\text{det}}|$ requirements. These probabilities are determined from the same multijet sample, but for $E_T < 15$ GeV, and are found to be $(0.0160 \pm 0.0016)\%$ for $|\eta^{\text{det}}| < 1.1$, and $(0.0622 \pm 0.0048)\%$ for $|\eta^{\text{det}}| > 1.5$. We normalize the integrated luminosity of the multijet sample so as to match the data sample used in the search for the signal, and correct for a small difference in trigger efficiency between the two samples.

The QCD $b\bar{b}$ background arises when both b quarks decay semileptonically to a muon, and one muon is misidentified as isolated. There are two ways for such events to mimic the signal. First, one of the b jets may not be reconstructed, and its muon can therefore appear to be isolated. Second, a muon can be emitted wide of its jet and be reconstructed as an isolated muon. The background from each source is measured using data collected with the same triggers as used for the muon signal. The events are required to pass all selections, except that the muon, which otherwise passes the isolated muon requirements, is within a jet. Events with truly isolated muons are excluded. Each event is then weighted by the probability that a nonisolated muon is reconstructed as an isolated one. This probability is measured using the same data sample, except for $E_T < 15$ GeV, and is found to be $(2.94 \pm 0.53)\%$ for the case of a ‘‘lost jet,’’ and $(1.38 \pm 0.25)\%$ for a ‘‘wide μ ,’’ for muons with $p_T < 32$ GeV. The probabilities are parametrized as a function of the muon p_T . We calculate a weighted average of the two results to obtain the number of expected background events.

The background from $W + \text{jets}$ is estimated by applying a set of tag-rate functions to untagged signal candidates that

pass all final event selections. These tag-rate functions are measured using multijet data and correspond to the relative probability that a jet of given E_T and η^{det} has a tagging muon, for two run periods when the muon chambers had different operating efficiencies. We then correct the samples for a small difference in trigger efficiency between untagged and tagged events. We also correct the muon channel by a factor of 0.688 ± 0.034 to account for the effect of the $\Delta\phi$ cutoff used to minimize cosmic ray backgrounds, a selection that cannot be applied directly. Finally, to avoid double counting, we subtract the fraction of events expected from $t\bar{t}$ and QCD backgrounds and single top quark signals. The remaining fraction of $W + \text{jets}$ in the untagged signal candidates is 66–92%, depending on the location of the electron or isolated muon.

The numbers of events expected for the two signals and three backgrounds are shown in Table I, together with the final numbers of events in the candidate data samples for the electron and muon channels.

To calculate limits on the cross sections for single top quark production in the s -channel and t -channel modes, we use the numbers of observed events, the signal acceptances and backgrounds, and the integrated luminosities. Covariance matrices are used to describe the correlated uncertainties on these quantities. We use a Bayesian approach, with a flat prior for the single top quark cross section and a multivariate Gaussian prior for the other quantities. We calculate the likelihood functions in each decay channel and combine them to obtain the following 95% confidence level upper limits:

$$\begin{aligned}\sigma(p\bar{p} \rightarrow tb + X) &< 39 \text{ pb} \\ \sigma(p\bar{p} \rightarrow tqb + X) &< 58 \text{ pb}\end{aligned}$$

To conclude, we have searched for electroweak production of single top quarks and find no evidence for such production. We set upper limits on the cross sections for s -channel production of tb and t -channel production of tqb . The limits are consistent with expectations from the standard model.

We are grateful to T. Stelzer, Z. Sullivan, S. Willenbrock, and C.-P. Yuan for valuable discussions on theoretical aspects of the analysis. We thank the staffs at Fermilab and at collaborating institutions for contributions to this work, and acknowledge support from the Department of Energy and National Science Foundation (USA), Commissariat à l’Energie Atomique and CNRS/Institut National de Physique Nucléaire et de Physique des Particules (France), Ministry for Science and Technology and Ministry for Atomic Energy (Russia), CAPES and CNPq (Brazil), Departments of Atomic Energy and Science and Education (India), Colciencias (Colombia), CONACyT (Mexico), Ministry of Education and KOSEF (Korea), CONICET and UBACyT (Argentina), A.P. Sloan Foundation, and the A. von Humboldt Foundation.

- [1] L. Demortier *et al.*, The Top Averaging Group, for the CDF and DØ Collaborations, Fermilab-TM-2084 (1999).
- [2] M. Jezabek and J. H. Kühn, Phys. Rev. D **48**, R1910 (1993); **49**, 4970(E) (1994).
- [3] CDF Collaboration, F. Abe *et al.*, Phys. Rev. Lett. **74**, 2626 (1995); DØ Collaboration, S. Abachi *et al.*, *ibid.* **74**, 2632 (1995).
- [4] DØ Collaboration, B. Abbott *et al.*, Phys. Rev. D **60**, 012001 (1999).
- [5] M. Gallinaro, for the CDF Collaboration, in the Proceedings of the 14th International Workshop on High Energy Physics and Quantum Field Theory, Moscow, Russia, 1999, p. 1, hep-ex/9912011.
- [6] S. S. D. Willenbrock and D. A. Dicus, Phys. Rev. D **34**, 155 (1986).
- [7] T. M. P. Tait and C.-P. Yuan, Phys. Rev. D **63**, 014018 (2001), and references therein.
- [8] G. V. Jikia and S. R. Slabospitsky, Phys. Lett. B **295**, 136 (1992).
- [9] M. C. Smith and S. Willenbrock, Phys. Rev. D **54**, 6696 (1996).
- [10] T. Stelzer, Z. Sullivan, and S. Willenbrock, Phys. Rev. D **56**, 5919 (1997); **58**, 094021 (1998).
- [11] A. P. Heinson, A. S. Belyaev, and E. E. Boos, Phys. Rev. D **56**, 3114 (1997).
- [12] DØ Collaboration, S. Abachi *et al.*, Nucl. Instrum. Methods Phys. Res. A **338**, 185 (1994).
- [13] The detector pseudorapidity η^{det} is defined as the pseudorapidity of the calorimeter cluster (electron or jet) or central track (muon) with respect to the center of the DØ detector, where $\eta^{\text{det}} = -\ln \tan(\theta^{\text{det}}/2)$, and θ^{det} is the polar angle relative to the proton direction. The pseudorapidity η and polar angle θ are defined with respect to the primary interaction point.
- [14] The cone radius of a jet is defined as $R = \sqrt{(\Delta\phi)^2 + (\Delta\eta)^2}$, where $\Delta\phi$, $\Delta\eta$ specify the width of the jet, and ϕ is the azimuthal angle around the beam axis.
- [15] The opening angle between a muon and jet is defined as $\Delta R = \sqrt{[\Delta\phi(\mu, \text{jet})]^2 + [\Delta\eta(\mu, \text{jet})]^2}$.
- [16] A. Pukhov *et al.*, hep-ph/9908288. We used CompHEP version 3.0.
- [17] G. Marchesini *et al.*, Comput. Phys. Commun. **67**, 465 (1992). We used HERWIG version 5.7.
- [18] T. Sjöstrand, Comput. Phys. Commun. **82**, 74 (1994). We used PYTHIA version 5.7 and JETSET version 7.4.
- [19] R. Brun *et al.*, CERN Program Library Writeup W5013, 1993. We used GEANT version 3.15.